
New Phantom Design for "Mapping" Spatial Resolution in SPECT Imaging

Daniel J. Bandy and Kimberlee J. Kearfott

Good Samaritan Regional Medical Center, Phoenix, Arizona and Georgia Institute of Technology, Atlanta, Georgia

A new phantom design to determine spatial resolution in Single Photon Emission Computed Tomography (SPECT) imaging systems is described. Specifically, spatial resolution in terms of full width at half maximum (FWHM) values can be determined simultaneously at multiple areas within the volumetric field of view. These values can then be assigned to their respective position or "mapped" within the field of view to demonstrate variations in spatial resolution.

The ultimate goal of nuclear medicine imaging procedures is to provide reliable, visual information about the organ system or biologic process being assessed. It is desirable to achieve the best possible images, each containing the maximum attainable information. This allows confident diagnostic interpretations to be made from the images. One specific factor affecting image quality is the spatial resolution of the imaging system. The most commonly used methods to determine spatial resolution are (a) use of transmission bar phantoms in conjunction with a cobalt sheet source for planar imaging and (b) three-dimensional fluid-filled phantoms containing various plexiglas inserts for single-photon emission computed tomography (SPECT) and positron emission tomography (PET) imaging. A third, more quantitative approach, is achieved by measuring the full width at half maximum (FWHM) value from the respective line spread function (LSF). These measurements can be made to evaluate either in-plane resolution or axial resolution (slice thickness). A disadvantage of using this technique in SPECT imaging is that the measurements are typically made with the source in one position within the field of view. It is then necessary to move the source to an additional position to make another measurement. Thus the spatial resolution measurements are only made at some specific distance from the center of the field of view and collecting additional information about positional variation in spatial resolution is time consuming.

The new tomographic phantom design, presented here, overcomes this disadvantage by representing the source as a thin, uniform, plane of radioactivity, tilted at a known angle, encompassing much of the field of view. Reconstructed sagittal slices yield thin lines of activity from which individual LSFs and, thus, FWHM values can be obtained anywhere

along the length of the slice. Thus, by evaluating a number of equidistant sagittal slices, the spatial resolution of the system can be easily and quickly evaluated at both multiple distances from the center of the field of view and at different axial positions throughout the volume. These values can be assigned to specific locations or "mapped" within the volumetric field of view.

MATERIALS AND METHODS

A supporting structure for the radioactive source was constructed from 2-mm thick plexiglas. A 30-cm square piece served as the base. To this, a 2-cm border of additional plexiglas was attached to the edges. This provided a small "lip" to prevent any leakage of radioactive solution from the source. A removable 26-cm square lid which fit within the border of the base served as a means to compress the absorbent paper containing the radioactive solution and to assure it was kept flat, thus maintaining a uniform source thickness. The base structure was affixed to two side pieces such that a 45° angle with respect to the scan table was achieved. This was done to simulate depth which occurs during actual patient acquisition (Fig. 1).

To image the phantom, 1 mCi (37 MBq) of technetium-99m (^{99m}Tc) as sodium pertechnetate was diluted to a volume of 20 cc with normal saline. A sheet of absorbent toweling was positioned within the bordered base of the phantom. The radioactive solution was then applied to all areas of the paper using a syringe with the needle removed. The solution was allowed to distribute over the toweling for 15 min to allow uniform dispersion. The plexiglas cover was then placed on top of the toweling. Slight pressure was applied to force any excess solution to the sides of the phantom and also to eliminate air pockets. The phantom was then centered on the imaging table and leveled using a small carpenter's level. The degree of uniform tracer dispersion was evaluated visually by placing the phantom in the field of view and acquiring a static image. No analysis was performed to quantitate uniformity. Several imaging parameters were used to evaluate the phantom and are detailed in Table 1. In all cases, the data were reconstructed using a Butterworth filter (Nyquist cutoff frequency = 0.6, Order = 5). The resulting 1 pixel-thick sagittal slices were numbered in order to select slices equidistant from each other for analysis. Slices at both edges, the center, and midpoint between the edges and center of the phantom, were

For reprints contact: Kimberlee J. Kearfott ScD, Georgia Institute of Technology, Atlanta, GA 30332-0225.

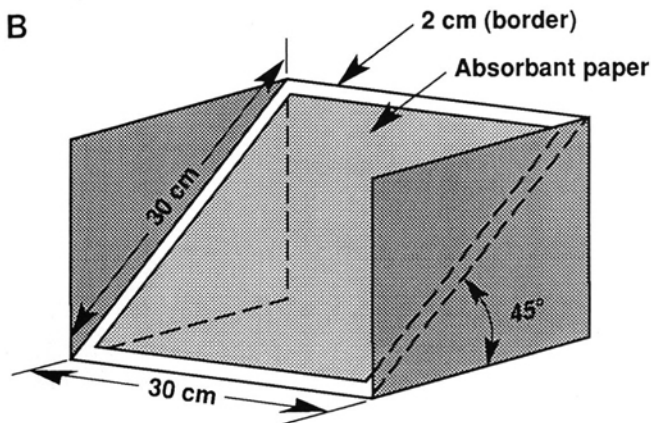
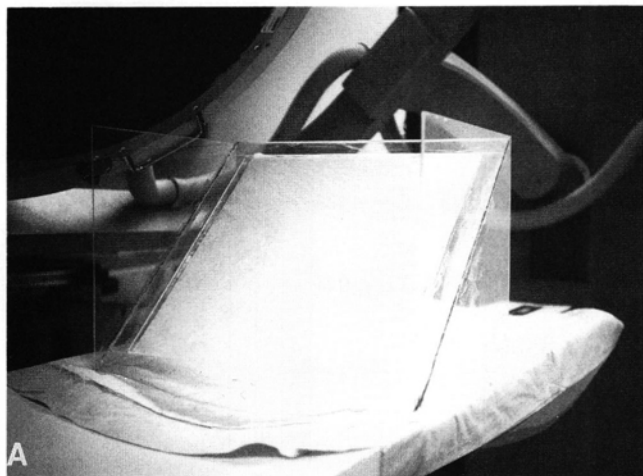


FIG. 1. (A) Tomographic phantom in position on imaging table. (B) Schematic representation of tomographic phantom.

used for analysis. Since pixel size had been previously determined to be 6.00 mm and 3.05 mm for a 64 and 128 word matrix, respectively, it was possible to assign the slices selected for analysis a numerical distance from the center of the field of view. These slices correspond to distances of 12.0 cm (edge slices), 6.0 cm (midpoint slice) and 0 cm (center slice) from the center of the field of view and represent in-plane spatial resolution values. From each slice, five similarly equidistant points, (top, bottom, center, midpoint between top and center, and midpoint between bottom and center of the phantom), were chosen to obtain LSFs and FWHM values. These positions correspond to distances of 8.4 cm (top and bottom points), 4.2 cm (midpoints), and 0 cm (center point) and represent axial spatial resolution values. Thus, a total of 25 measurements per imaging sequence were obtained.

RESULTS AND DISCUSSION

The measured spatial resolution values in terms of FWHM for the field of view occupied by the phantom have been mapped according to their respective positions and are displayed graphically in Figure 2. Regional averages are also reported in Table 2 in accordance with the schematic diagram presented as Figure 3. The total average spatial resolution values for the various collimators used are consistent with

TABLE 1. Imaging Sequences Used to Evaluate Phantom

Imaging [*] sequence	Collimator	Matrix (word)	Number of projections	Total rotation (degrees)
(1)	High resolution	64 × 64	64	360
(2)	High resolution	64 × 64	32	180
(3)	High resolution	128 × 128	64	360
(4)	High sensitivity	64 × 64	64	360
(5)	Leap	64 × 64	64	360
(6)	Medium-energy	64 × 64	64	360

^{*} In all sequences a time of 25 sec per image projection was used.

other studies which have evaluated the performance characteristics of these collimators in planar imaging with respect to spatial resolution (1). As the center of the field of view or tomographic volume is approached a general increase in FWHM value (loss of spatial resolution) is noted. In a previously reported study (2), a line source of radioactivity mounted inside a methacrylate tank was imaged to determine spatial resolution. A comparison of FWHM values was presented after an arithmetic or geometric mean of opposing detector profiles had been calculated. In both instances a loss of spatial resolution is noted at the center of the field of view as compared to the periphery. The new phantom design extends this principle into another dimension and allows simultaneous determination of spatial resolution within a plane and axially from a single data set.

The relatively coarse linear sampling in the 64 × 64 word matrix (pixel size = 6.02 mm) is adequate to allow the variations in spatial resolutions to be depicted without defining the limiting value the spatial resolution may achieve. To recover spatial frequencies in a signal up to the Nyquist frequency, a linear sampling distance needs to be \leq to $1/2 \times$ (Nyquist cutoff frequency) (3). For this study a Nyquist cutoff frequency of 0.6 cm^{-1} was used and thus a linear sampling distance of 0.83 cm (8.3 mm) is required. Therefore, the sampling distance of 6.02 mm provided by the 64 × 64 word matrix is suitable for these studies.

The phantom was not evaluated with a scattering or attenuating medium present at this time as it was desired only to demonstrate the variation of spatial resolution across the field of view. Thus, it was possible to maintain increased counting statistics relative to a constant scan time, provide more uni-

TABLE 2. Regional Spatial Resolution Values (FWHM in mm)

Imaging sequence	Outer perimeter average value (n = 16)	Inner perimeter average value (n = 8)	Center value (n = 1)	Total average value (n = 25)
(1)	14.5 ± 1.2	15.3 ± 1.0	17.4	14.5 ± 1.2
(2)	16.6 ± 0.3	16.9 ± 0.4	18.0	16.7 ± 0.4
(3)	9.5 ± 0.2	9.5 ± 0.3	10.5	9.6 ± 0.3
(4)	18.1 ± 0.6	20.0 ± 0.5	21.0	18.9 ± 1.2
(5)	15.2 ± 0.4	15.5 ± 0.5	16.2	15.3 ± 0.5
(6)	17.0 ± 0.9	19.4 ± 0.6	21.0	17.9 ± 1.5

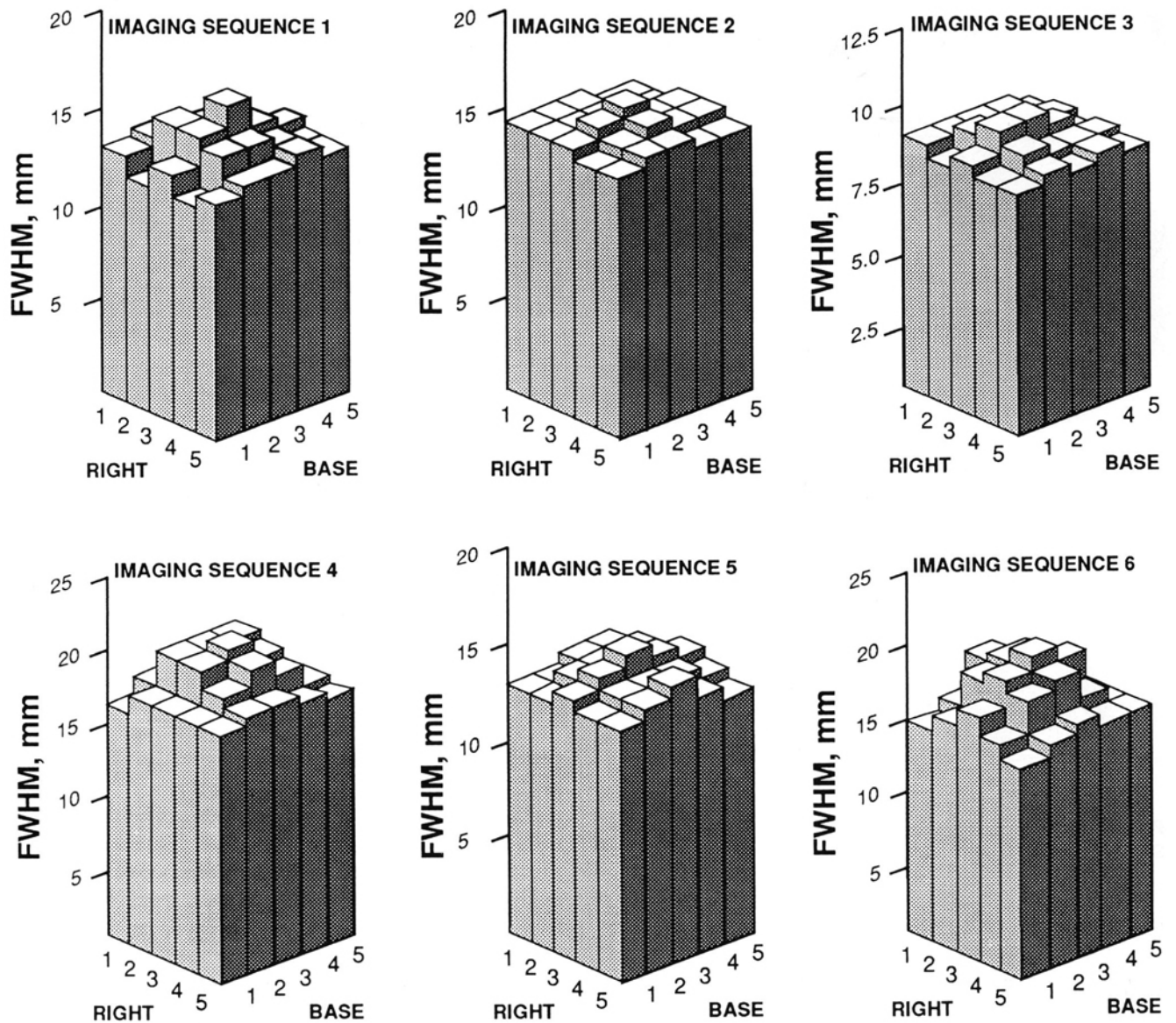


FIG. 2. Schematic maps of FWHM measurements for the imaging sequences presented in Table 1.

form counting statistics, and maximize any variations in spatial resolution. Scatter radiation primarily alters the PSF or LSF in the lower portions of the profile curve, specifically below the 50% level at which the FWHM is obtained. Therefore, for future studies, it is felt that measuring the full width at one-tenth of maximum (FWTM) would more accurately describe the effects of scatter on the spatial resolving powers of the system.

An attenuation medium would also increase the scatter component of the data set, and at the same time reduce the total number of counting statistics present in the resulting LSF. Neglecting the contribution of scatter from an attenuation medium, its effect on spatial resolution measurements should be minimal.

The importance of uniform spatial resolution has a profound influence on image reconstruction. Many reconstruction algorithms assume that each of the data points comprising a scan profile reflect the summed activity within a well

defined column of material through an object (3,4). If the nonuniformity of an imaging system is great, this assumption may not be entirely valid. This can lead to the degradation of images, usually in the form of image blurring or artifact production. Additionally, the quantitative accuracy of data may be altered due to variations in plane spatial resolution. This especially may be true when the object size approaches the resolution limits of the system and the effects due to partial volume are more pronounced.

CONCLUSION

The new phantom design allows for easy, simultaneous determination of spatial resolution (FWHM) at multiple areas within the volumetric field of view. Both axial and in-plane resolution values can be determined from a single data set without moving the phantom. This eliminates the need to

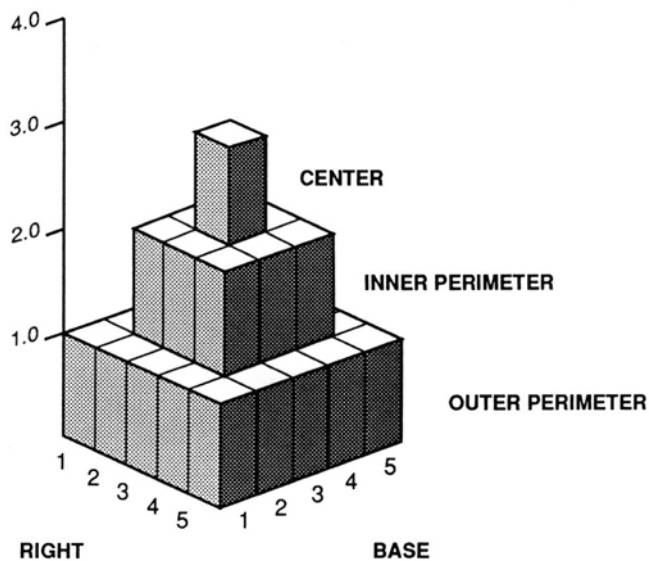


FIG 3. Regional division of schematic map depicting FWHM measurements. Each cell represents a single FWHM measurement. For the axis labeled RIGHT, cells 1 and 5 correspond to distances of 8.4 cm from the center of the field of view, 4.2 cm for cells 2 and 4, and 0 cm for cell 3. For the axis labeled BASE, the corresponding distances are 12.0 cm for cells 1 and 5, 6.0 cm for cells 2 and 4, and 0 cm for cell 3.

make multiple LSF measurements at discrete intervals; each requiring the line phantom to be repositioned.

In order to maximize the usefulness of the phantom, it is suggested that the physical dimensions be increased to further occupy the field of view. Additional testing should be conducted to quantitatively evaluate the initial radioisotope distribution in the phantom, demonstrate the effects from a scattering or attenuating medium, and compare the results to other phantoms, which evaluate similar parameters (i.e., single capillary tubes, spiral capillary tube phantom, or a three-line phantom).

The initial results indicate the phantom could be used on a periodic basis to monitor fine changes in spatial resolution throughout the volumetric field of view. Since the spatial resolution characteristics of an imaging system can be "mapped," it is postulated that the reconstruction algorithms could be tailored to a specific imaging system to eliminate a portion of the image degradation caused by nonuniform spatial resolution.

REFERENCES

1. Sorenson JA, Phelps ME. *Physics in nuclear medicine*. 2nd ed. Orlando, FL: Grune and Stratton, 1987:331-345.
2. Larsson SA. Gamma camera emission tomography. *Acta Radiol* 1980;363:5-75.
3. Sorenson JA, Phelps ME. *Physics in nuclear medicine*. 2nd ed. Orlando, FL: Grune and Stratton, 1987:401, 406, 413-419.
4. Rowland SW. Computer Implementation of Image Reconstruction Formulas. In: Herman GT, *Topics in applied physics, Volume 32: Image reconstruction from projections*. New York, NY. Springer-Verlag, 1979:9-78.